HHS Public Access

Author manuscript

ACS Chem Biol. Author manuscript; available in PMC 2019 November 16.

Published in final edited form as:

ACS Chem Biol. 2018 November 16; 13(11): 3065–3071. doi:10.1021/acschembio.8b00827.

Precise Small Molecule Degradation of a Noncoding RNA Identifies Cellular Binding Sites and Modulates an Oncogenic Phenotype

Yue Li and **Matthew D. Disney***

The Department of Chemistry, The Scripps Research Institute, Jupiter, Florida 33458, United States

Abstract

Herein, we describe the precise cellular destruction of an oncogenic noncoding RNA with a small molecule—bleomycin A5 conjugate, affording reversal of phenotype and a facile method to map the cellular binding sites of a small molecule. In particular, bleomycin A5 was coupled to a small molecule that selectively binds the microRNA-96 hairpin precursor (pri-miR-96). By coupling of bleomycin A5's free amine to the RNA binder, its affinity for binding to pri-miR-96 is >100-fold stronger than to DNA and the compound selectively cleaves pri-miR-96 in triple negative breast cancer (TNBC) cells. Indeed, selective cleavage of pri-miR-96 enhanced expression of FOXO1 protein, a proapoptotic transcription factor that miR-96 silences, and triggered apoptosis in TNBC cells. No effects were observed in healthy breast epithelial cells. Thus, conjugation of a small molecule to bleomycin A5's free amine may provide programmable control over its cellular targets. Few approaches are available to define the binding sites of small molecules within cellular RNAs. Our targeted cleavage method provides such an approach that is straightforward to implement. That is, we determined experimentally the site cleaved within pri-miR-96 *in vitro* and in cells; these studies revealed that the site of cleavage is the precise site for which the small molecule cleaver was designed and in agreement with modeling. These studies demonstrate the potential of sequence-based design to provide bioactive compounds that precisely recognize and cleave RNA in cells.

Graphical Abstract

*Corresponding Author Disney@scripps.edu.

ASSOCIATED CONTENT

Supporting Information

The Supporting Information is available free of charge on the ACS Publications website at DOI: 10.1021/acschem-bio.8b00827.

Primers used in this study, *in vitro* mapping gel, MST binding data, RT-qPCR data, cellular permeability data, apoptosis data, Sanger sequencing data, molecular modeling, and experimental procedures (PDF)

Notes

The authors declare no competing financial interest.

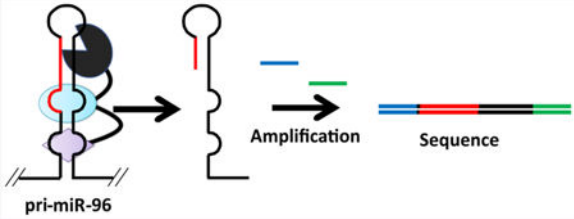

The ENCODE Project revealed that over 70% of our genome is transcribed into RNA.[1] These RNAs, particularly those that are noncoding, have diverse functions.[1] Small molecule targeting of RNA, however, has been challenging, except for RNAs that fold into globally ordered, highly defined three-dimensional structures such as ribosomes and riboswitches.[2–4] More recently, it has been shown that pre-mRNAs in complexes can be targeted and stabilized with small molecules.[5,6] Most RNAs, however, do not have highly complex long-range folds but do have extensive two-dimensional (secondary) structures including motifs such as hairpins, internal loops, and bulges that could be targeted with small molecules.[7,8] Indeed, small molecules have been discovered that target biological RNAs that contain these folds such as microRNA precursors (miRNAs).[9–11] Furthermore, approaches to study the cellular binding of small molecules to RNA targets are needed to support mechanism of action studies.

To provide rational approaches to target RNA with small molecules, we developed a sequence-based approach dubbed Inforna.[12] In particular, Inforna enabled the design of a small molecule (Targaprimir-96, 1, Figure 1A) that selectively targets the Drosha endonuclease processing site of oncogenic primary microRNA-96 (pri-miR-96).[13] MiRNAs are non-coding RNAs that play pervasive roles in biology, and their aberrant expression or mutation can be causative of disease. They are initially produced as precursors (pri-miRNA) that are processed by the nuclease Drosha followed by translocation to the cytoplasm as precursor microRNAs (pre-miRNAs). Pre-miRNAs are cleaved by the cytoplasmic nuclease Dicer to produce mature miRNAs that bind to the 3′ untranslated regions (UTRs) of mRNAs and repress translation. Application of **1** to triple negative breast cancer (TNBC) cells inhibited the production of mature miR-96, derepressed proapoptotic transcription factor Forkhead box protein O1 (FOXO1) that the miRNA repressed, and triggered apoptosis (Figure 1B).[13]

To expand the functional repertoire of small molecules that target RNA from simple binding to selective cleavage, bleomycin A5 was conjugated to **1**, affording **2** (Figure 1). Bleomycin, a natural product used for treatment of cancer, cleaves DNA[14,15] but also cleaves RNA, as pioneered by the Hecht group.[16,17] Bleomycin contains four domains: (i) a metal ion-binding domain that activates O_2 and leads to nucleic acid cleavage;[18–21] (ii) a DNA-binding domain, which affects cleavage efficiency;[22] (iii) a linker region between the metal ion-binding and DNA-binding domains, which also affects cleavage efficiency;[23–27] and (iv) a carbohydrate domain that facilitates cellular uptake.[20] We chose bleomycin A5 as the cationic dimethyl sulfonium in the C-terminal DNA-binding domain has been replaced with a butyl-1,4-diamine side chain. This modification serves two purposes: (i) facile conjugation of the terminal primary amine to RNA-binding modules containing carboxylates; notably,

acylation of the butyl-1,4-diamine side chain (cationic) with a small molecule affords an uncharged linkage; and (ii) reduction of DNA binding affinity,[28–30] as the cationic side chain, known to drive binding to DNA, has been acylated and is no longer charged. In addition, it has been shown that increasing the size and hydrophobicity of bleomycin A5's butyl-1,4-diamine side chain further decreases DNA binding affinity and the extent of cleavage.[28–30] Conjugation of an RNA-binding module is therefore likely to alter bleomycin A5's binding and cleavage preferences toward RNA, as we have observed in the selective cleavage of expanded r(CUG) repeats.[31]

The secondary structure of oncogenic pri-miR-96[32] was analyzed to determine if it might be a suitable target for bleomycin-mediated cleavage (Figure 1B). Previously, it has been shown that bleomycin can cleave AU pairs in RNA,[33] and indeed AU pairs are present adjacent to pri-miR-96's Drosha site. Thus, conjugation of bleomycin to compound **1** could provide a selective cleaving small molecule, provided that the bleomycin is positioned toward these AU pairs. As previous studies have shown that the 3,5-di-*tert*-butylbenzyl benzimidazole module in 1 binds the 1 X 1 UU internal loop in the Drosha site (teal oval; Figure 1),[12] conjugation of bleomycin A5 to **1** (**2**; Figure 1A) places the cleaving module near the neighboring AU pairs. Control compound **3** (Figure 1A), which lacks the RNA-binding modules, was also synthesized.

The sites of cleavage by **2** and **3** were studied *in vitro* by using primer extension with a radioactively labeled primer after reaction (Figure S1). In the presence of **2** and Fe^{2+}, a site of selective cleavage was observed adjacent to the Drosha site, as predicted; that is, cleavage at this site was not observed when pri-miR-96 was treated with Fe^{2+} alone or **3** and Fe^{2+} (Figure S1). (Note: Bands that appear in the "0" (untreated) and "Fe^{2+}" (treated solely with Fe^{2+}) were not considered as they are due to "RT stops" and not to compound treatment.) To further assess the ability of **2** and **3** to cleave nucleic acids, they were tested for cleaving DNA. As shown in Figure 2A, **2** cleaved DNA with 5-fold lower efficiency than **3** at concentrations ≥500 nM, as calculated by comparing the percentage of DNA plasmid cleaved by both compounds ($p < 0.05$). Thus, conjugation of bleomycin to an RNA binder significantly reduced its ability to cleave DNA *in vitro,* as expected based on previous reports.[30] To confirm our *in vitro* cleavage results, we measured the affinities of **1**, **2**, **3**, and bleomycin A5 for pri-miR-96 and DNA by microscale thermophoresis (MST;[34,35] Figure 2B). In agreement with *in vitro* cleavage studies, **1** and **2** bound avidly to pri-miR-96 with K_d's of 39 ± 18 nM and 64 ± 11 nM, respectively, while saturable binding to **3** and bleomycin A5 was not observed ($K_d > 30\ \mu M$). In contrast, no saturable binding of **1**, **2**, or **3** to DNA was observed ($K_d > 30 \mu M$); however, bleomycin A5 bound DNA with a K_d of ~1 μM. Collectively, these results indicate that modification of bleomycin A5's side chain, whether by an RNA-binding module or a peptoid linker, greatly reduced its affinity for DNA as expected[30] and that 2 selectively bound pri-miR-96 in the low nanomolar concentration range.

This phenomenon was also observed in cells, as studied by assessing DNA damage using an antibody for the gamma H2A histone family, member X (γ-H2A.X),[36] a marker for DNA double stranded breaks visualized as nuclear foci. In agreement with *in vitro* DNA cleavage (Figure 2A), **3** caused ~2.3-fold more DNA damage than 2 (500 nM of **2** or **3**; Figure 2C), as

calculated by comparing the average foci number per cell for each compound. Collectively, these data show that pri-miR-96 can be cleaved to a greater extent by **2** than DNA is cleaved within a concentration window; that is, the targets that are cleaved by bleomycin can be attenuated by addition of an RNA-binding module at midnanomolar concentrations both *in vitro* and in cells, *vide infra.*

Next, the effect of **2** on pri-miR-96 and mature miR-96 levels in MDA-MB-231 TNBC cells was measured via RT-qPCR To study the cleaving effects of **2**, the compound was first complexed with Fe^{2+} (1 equiv), diluted into growth medium, and then added to cells. While both compounds reduced mature miR-96 levels (Figure 3A), 1 increased the level of primiR-96, while **2** decreased it (Figure 3B), as expected based on their designed mode of action, simple binding and cleavage, respectively. When **2** was prepared in the absence of Fe^{2+}, no statistically significant effect was observed on pri-miR-96 levels (Figure S3); mature miR-96 levels were reduced upon treatment with 500 nM compound as expected based on **2**'s binding properties ($p < 0.05$). These data suggest that the cleavage of pri-miR-96 contributes to the downregulation of mature miR-96. Control compound **3** had no effect on mature or pri-miR-96 levels (Figure S4). To further confirm **2**'s mode of action, a competition cleavage experiment was completed in which increasing concentrations of **1** and a constant concentration of **2** were delivered to MDA-MB-231 cells. [Note: both compounds show similar levels of cell permeability at 500 nM as determined by flow cytometry (Figure S5).] Results show that the cleavage caused by **2** is effectively competed off when **1** was added (Figure 3C). Each of these results supports the hypothesis that 2 is targeting primiR-96 for destruction.

In cancer cells, miR-96 suppresses apoptosis by silencing the production of pro-apoptotic transcription factor FOXO1.[32] Thus, inhibition of miR-96 by **2** should increase the amount of FOXO1 and trigger apoptosis. Indeed, the amount of FOXO1 protein in MDA-MB-231 cells was increased by ~1.8-fold when treated with 500 nM of **2** (Figure 3D). The effect of **2** on phenotype (suppression of apoptosis)[12,13,32] was then assessed by using both Annexin/PI staining and Caspase assays. Importantly, **2** induced apoptosis in MDA-MB-231 cells (Figure 3E (red) and Figure S6) and had no effect on MCF- 10a healthy breast epithelial cells in which pri-miR-96 is not expressed in measurable amounts (Figure 3E, blue). Further, the apoptotic effect of **2** was reduced in cells in which pri-miR-96 was overexpressed from a plasmid (Figure 3E, green). We also measured the effect of **2** on other miRNAs, including miR-10b, which was previously shown to be a target of bleomycin A5,[33] oncogenic miR-21,[37] and all other miRNAs predicted to target the FOXO1 3′untranslated region (UTR) by TargetScan.[38] None of these targets was affected (Figure S7).

One of the beauties of antisense is that the oligonucleotide's on- and off-targets can be inferred by depletion of an RNA's levels. To determine whether **2** can be used in target profiling studies akin to antisense, an unbiased profiling experiment (RiboSNAP; small molecule nucleic acid profiling by cleavage applied to RNA) on the 349 miRNAs expressed in MDA-MB-231 cells was completed. The data from these studies are presented as a volcano plot, a logarithmic plot of fold change vs statistical significance (Figure 4A). Importantly, these studies show (i) miR-96 levels were affected to the greatest extent and were the most statistically significant, illustrating **2**'s remarkable selectivity. This result is of

great interest considering that **2**'s mode of action is RNA cleavage. Evidently, conjugation of bleomycin A5 to **1** does not alter **1**'s selectivity;[13] (ii) small molecule-bleomycin conjugates can be used in cellular target profiling studies; and (iii) the RNA targets cleaved in cells by bleomycin can be precisely programmed by conjugation to a selective RNA small molecule binder. One challenge in developing chemical probes targeting RNA has been the perception that compounds cannot be selective, and these studies suggest that small molecules, even those that cleave, can be selective for an RNA target.

The most common method to identify small molecule binding sites within an RNA is to monitor sites of protection from nuclease cleavage or reaction with chemical modification reagents. Indeed, this approach identified sites in the ribosome that bound antibiotics.[39,40] However, some binding sites can be silent due to a lack of reactivity with a chemical modifier and can require long residence times of the small molecule to prevent reactivity (irreversible). Thus, careful tuning of the experimental conditions is often necessary. Although laborious, these types of experiments are invaluable to validate or identify the target(s) of small molecules, which is essential to establish a compound's mode of action.

We posited that analyzing the cleavage footprints of **2** from RNA harvested from treated cells could identify the precise binding site, an approach we named Ribo-SNAP-Map. If cleavage sites could be amplified, both the small molecule's RNA target (Ribo-SNAP) and the binding site within the RNA (Ribo-SNAP-Map) could be identified quickly after compound treatment. To implement Ribo-SNAP-Map, we developed a procedure to enrich the partial cleavage products of pri-miR-96 (Figure 4B) using a gene specific forward primer and a universal reverse primer in an RT-qPCR experiment.[41] Gel analysis showed a new band at ca. 130 base pairs only when cells were exposed to **2**, not to **1** or **3** (Figure S8). Sequencing analysis confirmed that the cleavage sites were proximal to the predicted and *in vitro* mapped binding sites for **2** (Figure 4C and Figure S8). Molecular modeling of **2** binding with pri-miR-96 (Figure S9) also showed that **2** positions the cleaving moiety toward the AU sequence that is cleaved rather than other regions in the RNA that are distant from the ligand's binding site. Thus, Ribo-SNAP-Map can indeed be used to map binding sites in cells. Notably, AU pairs proximal to a small molecule's binding site is not required for selective cleavage of bleomycin A5 conjugates, as observed for r(CUG) repeats.[31]

Previous studies have provided small molecules that cleave RNA by using light,[42] are nuclease mimics,[43] or recruit endogenous nucleases to an RNA target.[44] In the first approach, applicability can be limited because of the necessity of light to penetrate cells and tissue. Compounds that act as nuclease mimics interact with an expanded repeating RNA and have a mixed mode of inhibition (transcriptional inhibition, inhibition of protein binding, and cleavage).[43] Notably, expanded repeating RNAs are atypical targets; due to its repeating nature and hence multiple small molecule binding sites, inefficient cleavage could afford a significant biological effect. More recently, we developed an approach named ribonuclease targeting chimeras (RIBOTACs) to recruit endogenous RNase L to cleave a desired RNA target.[44] However, cleavage patterns on the RNA target using each of these three methods can be complex and may not be proximal to the binding site. In contrast, cleavage with **2** is proximal and not complex, allowing straightforward identification of RNA sequences nearby ligand binding sites.

Herein, we showed that small molecules can be engendered with antisense-like properties in cells using chimeric compounds comprised of a selective RNA-binding small molecule and bleomycin A5 as a cleaving moiety. Indeed, these studies and others suggest that (i) the targets cleaved by bleomycin can be tuned by conjugation to an RNA-binding small molecule; (ii) these capacities are likely programmable; and (iii) the ability to cleave RNAs with small molecules could expand the target scope of ligands that modulate the biology of RNA, akin to the revolution that PROTACs[45] initiated in the protein targeting field. Most RNAs' biology may not be affected by simple binding and engendering a small molecule with the ability to cleave will likely expand the number of RNAs that can be targeted with organic compounds.

Supplementary Material

Refer to Web version on PubMed Central for supplementary material.

ACKNOWLEDGMENTS

This work was funded by the National Institutes of Health (R01 GM97455). We thank S. Velagapudi for help with initial studies and J. Childs-Disney for critical review of the manuscript. We thank H. Park of the X-ray Crystallography Core at Scripps Florida for Pymol modeling.

REFERENCES

(1). The ENCODE Project Consortium. (2012) An integrated encyclopedia of DNA elements in the human genome. Nature 489, 57–74,. [PubMed: 22955616]

(2). Tenson T, and Mankin A (2006) Antibiotics and the ribosome. Mol. Microbiol. 59, 1664–1677. [PubMed: 16553874]

(3). Howe JA, Wang H, Fischmann TO, Balibar CJ, Xiao L, Galgoci AM, Malinverni JC, Mayhood T, Villafania A, Nahvi A, Murgolo N, Barbieri CM, Mann PA, Carr D, Xia E, Zuck P, Riley D, Painter RE, Walker SS, Sherborne B, de Jesus R, Pan W, Plotkin MA, Wu J, Rindgen D, Cummings J, Garlisi CG, Zhang R, Sheth PR, Gill CJ, Tang H, and Roemer T (2015) Selective small-molecule inhibition of an RNA structural element. Nature 526, 672–677. [PubMed: 26416753]

(4). Ratmeyer LS, Vinayak R, Zon G, and Wilson WD (1992) An ethidium analogue that binds with high specificity to a base-bulged duplex from the TAR RNA region of the HIV-I genome. J. Med. Chem. 35, 966–968. [PubMed: 1548686]

(5). Naryshkin NA, Weetall M, Dakka A, Narasimhan J, Zhao X, Feng Z, Ling KK, Karp GM, Qi H, Woll MG, Chen G, Zhang N, Gabbeta V, Vazirani P, Bhattacharyya A, Furia B, Risher N, Sheedy J, Kong R, Ma J, Turpoff A, Lee CS, Zhang X, Moon YC, Trifillis P, Welch EM, Colacino JM, Babiak J, Almstead NG, Peltz SW, Eng LA, Chen KS, Mull JL, Lynes MS, Rubin LL, Fontoura P, Santarelli L, Haehnke D, McCarthy KD, Schmucki R, Ebeling M, Sivaramakrishnan M, Ko CP, Paushkin SV, Ratni H, Gerlach I, Ghosh A, and Metzger F (2014) Motor neuron disease. SMN2 splicing modifiers improve motor function and longevity in mice with spinal muscular atrophy. Science 345, 688–693. [PubMed: 25104390]

(6). Palacino J, Swalley SE, Song C, Cheung AK, Shu L, Zhang X, Van Hoosear M, Shin Y, Chin DN, Keller CG, Beibel M, Renaud NA, Smith TM, Salcius M, Shi X, Hild M, Servais R, Jain M, Deng L, Bullock C, McLellan M, Schuierer S, Murphy L, Blommers MJ, Blaustein C, Berenshteyn F, Lacoste A, Thomas JR, Roma G, Michaud GA, Tseng BS, Porter JA, Myer VE, Tallarico JA, Hamann LG, Curtis D, Fishman MC, Dietrich WF, Dales NA, and Sivasankaran R (2015) SMN2 splice modulators enhance U1-pre-mRNA association and rescue SMA mice. Nat. Chem. Biol. 11, 511–517. [PubMed: 26030728]

(7). Lu Z, and Chang HY (2016) Decoding the RNA structurome. Curr. Opin. Struct. Biol. 36, 142–148. [PubMed: 26923056]

(8). Bevilacqua PC, Ritchey LE, Su Z, and Assmann SM (2016) Genome-wide analysis of RNA secondary structure. Annu. Rev. Genet. 50, 235–266. [PubMed: 27648642]

(9). Im K, Song J, Han YT, Lee S, Kang S, Hwang KW, Min H and Min KH (2017) Identification of aminosulfonylarylisox- azole as microRNA-31 regulators. PLoS One 12, e0182331. [PubMed: 28783765]

(10). Yan H, Bhattarai U, Song Y, and Liang FS (2018) Design, synthesis and activity of light deactivatable microRNA inhibitor. Bioorg. Chem. 80, 492–497. [PubMed: 29990897]

(11). Yan H, Bhattarai U, Guo ZF, and Liang FS (2017) Regulating miRNA-21 biogenesis by bifUnctional small molecules. J. Am. Chem. Soc. 139, 4987–4990.

(12). Velagapudi SP, Gallo SM, and Disney MD (2014) Sequence-based design of bioactive small molecules that target precursor microRNAs. Nat. Chem. Biol. 10, 291–297. [PubMed: 24509821]

(13). Velagapudi SP, Cameron MD, Haga CL, Rosenberg LH, Lafitte M, Duckett DR, Phinney DG, and Disney MD (2016) Design of a small molecule against an oncogenic noncoding RNA. Proc. Natl. Acad. Sci U. S. A. 113, 5898–5903. [PubMed: 27170187]

(14). Sugiyama H, Kilkuskie RE, Chang LH, Ma LT, Hecht SM, Vandermarel GA, and Vanboom JH (1986) DNA strand scission by bleomycin - catalytic cleavage and strand selectivity. J. Am. Chem. Soc. 108, 3852–3854.

(15). Sugiyama H, Kilkuskie RE, Hecht SM, Vandermarel GA, and Vanboom JH (1985) An efficient, site-specific DNA target for bleomycin. J. Am. Chem. Soc. 107, 7765–7767.

(16). Carter BJ, de Vroom E, Long EC, van der Marel GA, van Boom JH, and Hecht SM (1990) Site-specific cleavage of RNA by Fe(ll).bleomycin. Proc. Natl. Acad. Sci. U. S. A. 87, 9373–9377. [PubMed: 1701259]

(17). Abraham AT, Lin JJ, Newton DL, Rybak S, and Hecht SM (2003) RNA cleavage and inhibition of protein synthesis by bleomycin. Chem. Biol. 10, 45–52. [PubMed: 12573697]

(18). Burger RM (1998) Cleavage of nucleic acids by bleomycin. Chem. Rev. 98, 1153–1170. [PubMed: 11848928]

(19). Hecht SM (1986) The chemistry of activated bleomycin. Acc. Chem. Res. 19, 383–391.

(20). Kane SA, and Hecht SM (1994) Polynucleotide recognition and degradation by bleomycin. Prog. Nucleic Acid Res. Mol. Biol. 49, 313–352. [PubMed: 7532315]

(21). Stubbe J, and Kozarich JW (1987) Mechanisms of bleomycin-induced DNA degradation. Chem. Rev. 87, 1107–1136.

(22). Berry DE, Chang LH, and Hecht SM (1985) DNA damage and growth inhibition in cultured human cells by bleomycin congeners. Biochemistry 24, 3207–3214. [PubMed: 2411288]

(23). Boger DL, Colletti SL, Honda T, and Menezes RF (1994) Total synthesis of Bleomycin A2 and related agents. 1. Synthesis and DNA binding properties of the extended C-terminus: tripeptide S, tetrapeptide S, pentapeptide S, and related agents. J. Am. Chem. Soc. 116, 5607–5618.

(24). Boger DL, Colletti SL, Teramoto S, Ramsey TM, and Zhou J (1995) Synthesis of key analogs of bleomycin A2 that permit a systematic evaluation of the linker region: identification of an exceptionally prominent role for the L-threonine substituent. Bioorg. Med. Chem. 3, 1281–1295. [PubMed: 8564421]

(25). Boger DL, Ramsey TM, Cai H, Hoehn ST, and Stubbe J (1998) Definition of the effect and role of the bleomycin A2 valerate substituents: preorganization of a rigid, compact conformation implicated in sequence-selective DNA cleavage. J. Am. Chem. Soc. 120, 9149–9158.

(26). Otsuka M, Masuda T, Haupt A, Ohno M, Shiraki T, Sugiura Y, and Maeda K (1990) Synthetic studies on antitumor antibiotic, bleomycin. 27. Man-designed bleomycin with altered sequence specificity in DNA cleavage. J. Am. Chem. Soc. 112, 838–845.

(27). Owa T, Haupt A, Otsuka M, Kobayashi S, Tomioka N, Itai A, Ohno M, Shiraki T, Uesugi M, Sugiura Y, and Maeda K (1992) Man-designed bleomycins: significance of the binding sites as enzyme models and of the stereochemistry of the linker moiety. Tetrahedron 48, 1193–1208.

(28). Ma Q, Xu Z, Schroeder BR, Sun W, Wei F, Hashimoto S, Konishi K, Leitheiser CJ, and Hecht SM (2007) Biochemical evaluation of a 108-member deglycobleomycin library: viability of a selection strategy for identifying bleomycin analogues with altered properties. J. Am. Chem. Soc. 129, 12439–12452. [PubMed: 17887752]

(29). Thomas CJ, Chizhov AO, Leitheiser CJ, Rishel MJ, Konishi K, Tao ZF, and Hecht SM (2002) Solid-phase synthesis of bleomycin A(5) and three monosaccharide analogues: exploring the role of the carbohydrate moiety in RNA cleavage. J. Am. Chem. Soc. 124, 12926–12927. [PubMed: 12405801]

(30). Xu ZD, Wang M, Xiao SL, Liu CL, and Yang M (2003) Synthesis, biological evaluation and DNA binding properties of novel bleomycin analogues. Bioorg. Med. Chem. Lett. 13, 2595–2599. [PubMed: 12852974]

(31). Rzuczek SG, Colgan LA, Nakai Y, Cameron MD, Furling D, Yasuda R, and Disney MD (2017) Precise small- molecule recognition of a toxic CUG RNA repeat expansion. Nat. Chem. Biol. 13, 188–193. [PubMed: 27941760]

(32). Guttilla IK, and White BA (2009) Coordinate regulation of FOXO1 by miR-27a, miR-96, and miR-182 in breast cancer cells. J. Biol. Chem. 284, 23204–23216. [PubMed: 19574223]

(33). Angelbello AJ, and Disney MD (2018) Bleomycin can cleave an oncogenic noncoding RNA. ChemBioChem 19, 43–47. [PubMed: 29084369]

(34). Moon MH, Hilimire TA, Sanders AM, and Schneekloth JS, Jr. (2018) Measuring RNA-ligand interactions with microscale thermophoresis. Biochemistry 57, 4638–4643. [PubMed: 29327580]

(35). Jerabek-Willemsen M, Wienken CJ, Braun D, Baaske P, and Duhr S (2011) Molecular interaction studies using microscale thermophoresis. Assay Drug Dev. Technol 9, 342–353. [PubMed: 21812660]

(36). Lane SIR, Morgan SL, Wu T, Collins JK, Merriman JA, ElInati E, Turner JM, and Jones KT (2017) DNA damage induces a kinetochore-based ATM/ATR-independent SAC arrest unique to the first meiotic division in mouse oocytes. Development 144, 3475–3486. [PubMed: 28851706]

(37). Esquela-Kerscher A, and Slack FJ (2006) Oncomirs - microRNAs with a role in cancer. Nat. Rev. Cancer 6, 259–269. [PubMed: 16557279]

(38). Agarwal V, Bell GW, Nam JW, and Bartel DP (2015) Predicting effective microRNA target sites in mammalian mRNAs. eLife 4, No. e05005, DOI: 10.7554/eLife.05005.

(39). Stern S, Moazed D, and Noller HF (1988) Structural analysis of RNA using chemical and enzymatic probing monitored by primer extension. Methods Enzymol 164, 481–489. [PubMed: 2468070]

(40). Moazed D, and Noller HF (1987) Interaction of antibiotics with functional sites in 16S ribosomal-RNA. Nature 327, 389–394. [PubMed: 2953976]

(41). Kwok CK, Ding Y, Tang Y, Assmann SM, and Bevilacqua PC (2013) Determination of in vivo RNA structure in low-abundance transcripts. Nat. Commun. 4, 2971. [PubMed: 24336128]

(42). Guan L, and Disney MD (2013) Small-molecule-mediated cleavage of RNA in living cells. Angew. Chem. Int. Ed. Eng. 52, 1462–1465.

(43). Nguyen L, Luu LM, Peng S, Serrano JF, Chan HY, and Zimmerman SC (2015) Rationally designed small molecules that target both the DNA and RNA causing myotonic dystrophy type 1. J. Am. Chem. Soc. 137, 14180–14189. [PubMed: 26473464]

(44). Costales MG, Matsumoto Y, Velagapudi SP, and Disney MD (2018) Small molecule targeted recruitment of a nuclease to RNA. J. Am. Chem. Soc. 140, 6741–6744. [PubMed: 29792692]

(45). Gu S, Cui D, Chen X, Xiong X, and Zhao Y (2018) PROTACs: an emerging targeting technique for protein degradation in drug discovery. BioEssays 40, 1700247.

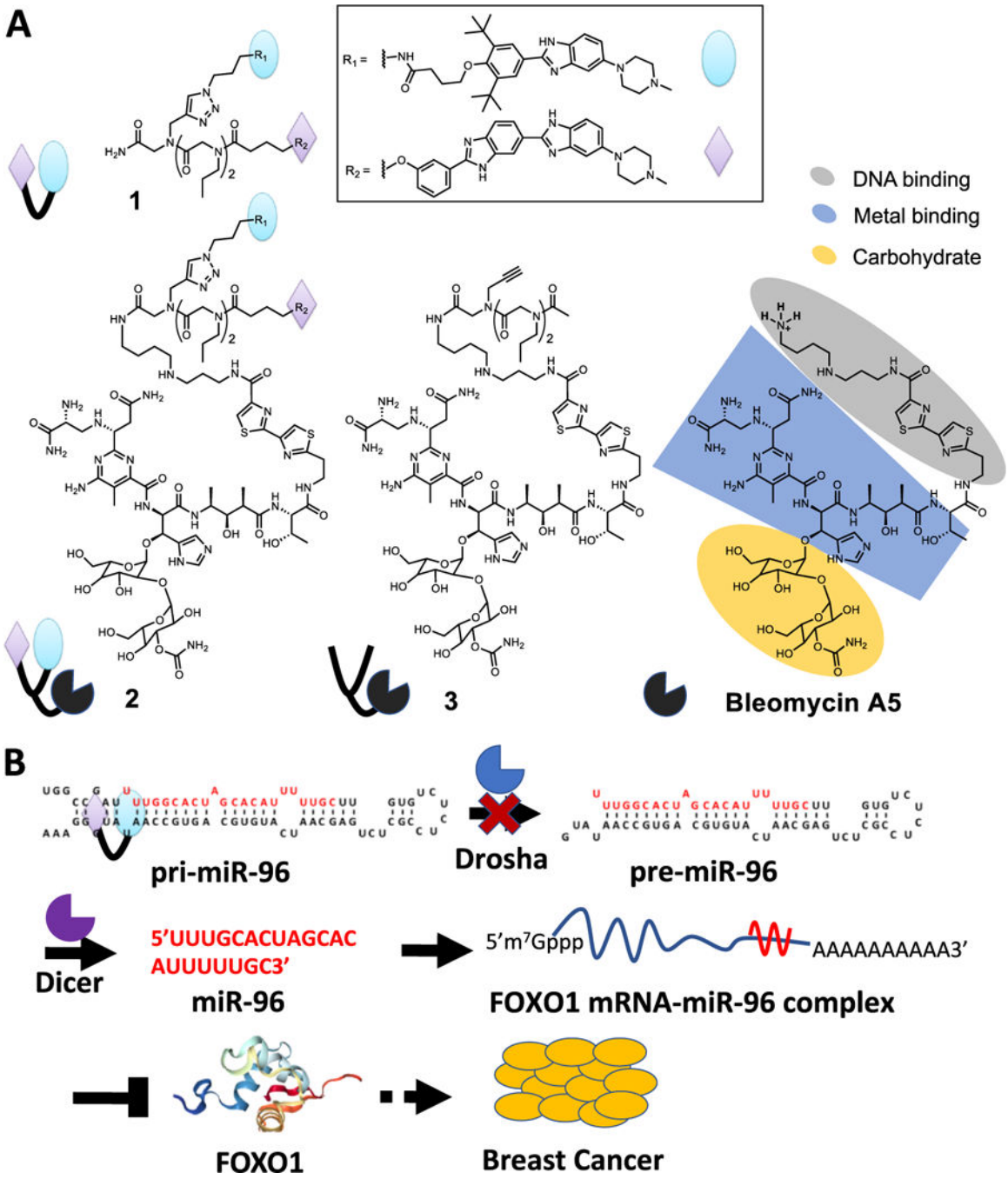

Figure 1.

Pri-miR-96 is oncogenic and suppresses apoptosis in cancer cells via repression of the pro-apoptotic transcription factor Forkhead box protein O1 (FOXO1). (A) Structures of the compounds used in these studies. Compound **1** was designed via Inforna and selectively targets primiR-96. Compound **2** is a version of **1** conjugated to bleomycin A5, while compound **3** is a version of **2** that lacks RNA-binding modules. (B) Secondary structure of pri-miR-96 and the miR-96-FOXO1 pathway. Compound binding sites are indicated in the secondary structure, and mature miR-96 is indicated in red lettering. The red "X" indicates

inhibition of Drosha processing by a small molecule and subsequent downstream steps. In previous studies, we showed that **1** inhibited the production of mature miR-96, derepressed a downstream target, pro-apoptotic transcription factor FOXO1, and triggered apoptosis.

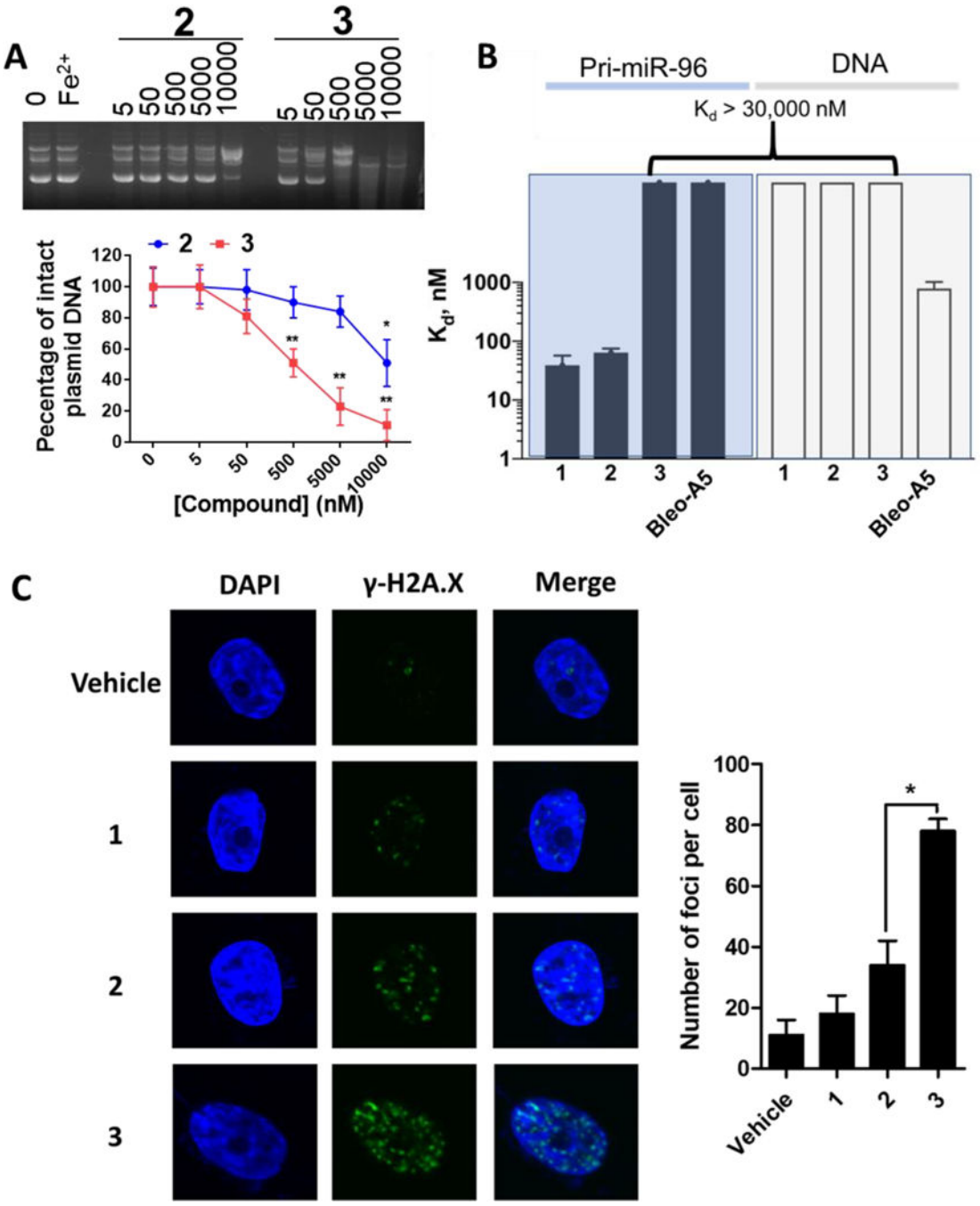

Figure 2.

Conjugation of a selective RNA binder to bleomycin A5 attenuates DNA cleavage *in vitro* and in cells. (A) Studying the DNA cleaving activity of **2** and **3** *in vitro*. Appending RNA-binding modules onto the bleomycin core (affording **2**) decreased the amount of DNA cleavage as compared to **3**, which lacks RNA-binding modules. (B) Affinities of **1**, **2**, **3**, and bleomycin A5 for Cy5-labeled pri-miR-96 or a Cy5-labeled AT-rich DNA hairpin, as determined by MST. (C) Visualization and quantification of DNA damage in MDA-MB-231 cells treated with 500 nM of **1**, **2**, or **3** for 12 h. Data are expressed as mean ± SEM (n ≥ 3).

*$p < 0.05$; **$p < 0.01$ as determined by a two-tailed Student *t* test by comparison to untreated DNA (B) or cells (C).

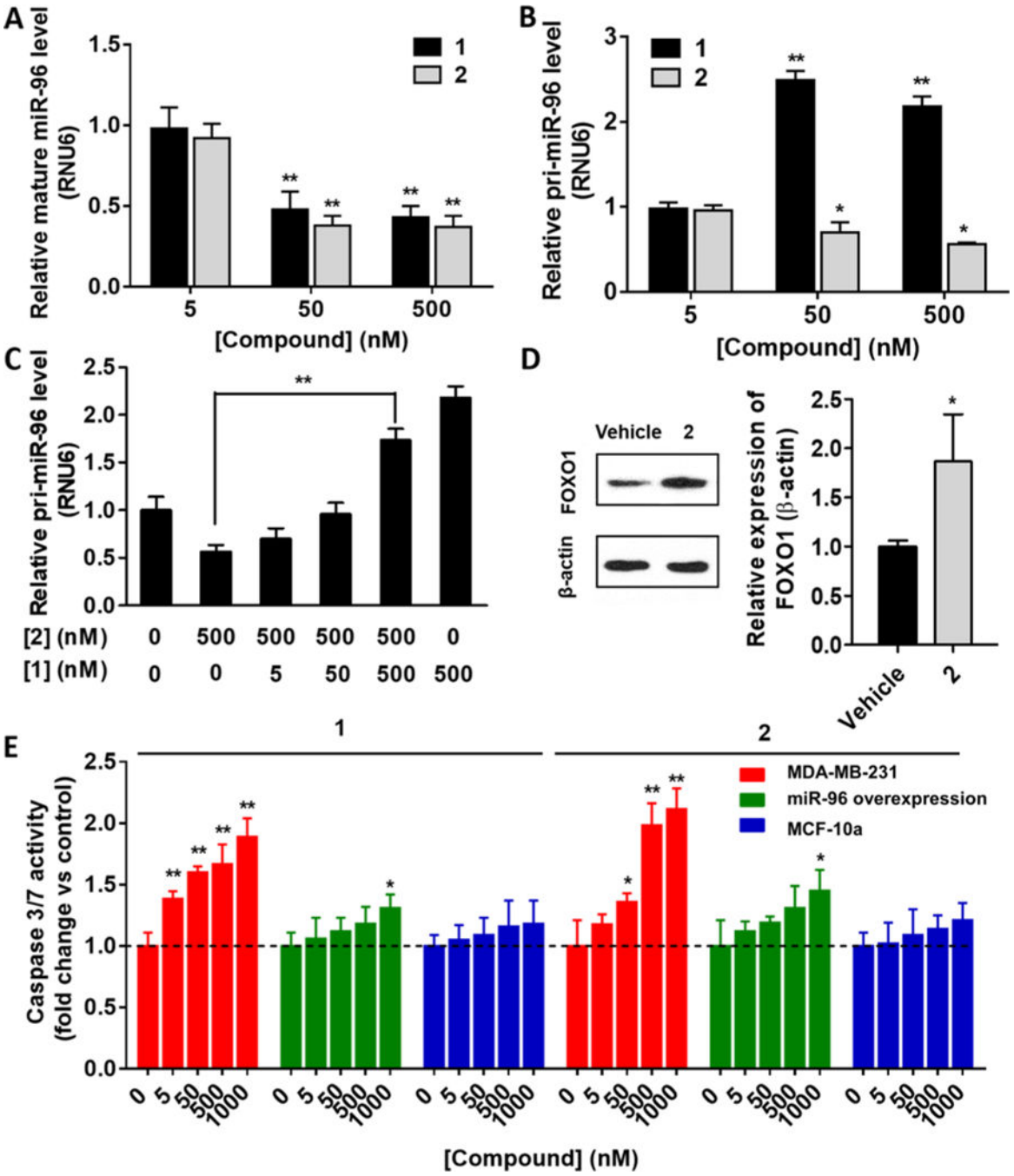

Figure 3.

Studying the effect of **1** and **2** on mature miR-96 and pri-miR-96 levels and on miRNA-mediated biology. (A) Effects of **1** and **2** on mature miR-96 levels in MDA-MB-231 TNBC cells, as determined by RT-qPCR. (B) Effects of 1 and 2 on pri-miR-96 levels in MDA-MB-231 cells. As expected based on their modes of action, **1** (simple binding) increased pri-miR-96 levels, while **2** (cleavage) reduced them. (C) Co-addition of increasing concentrations of **1** (5 to 500 nM) and a constant concentration of **2** (500 nM) to MDA-MB-231 cells increased levels of pri-miR-96, diminishing the cleaving capacity of **2** as

expected. (D) Effect of **2** on expression of FOXO1 protein, a direct target of miR-96, as determined by Western blot. (E) Effect of **1** or **2** on apoptosis in MDA-MB-231 cells (red), MDA-MB-231 cells that overexpress pri-miR-96 *via* a plasmid (green), and in MCF-10a healthy breast epithelial cells (blue), as determined by Caspase assays. Data are expressed as mean ± SEM ($n > 3$). $*p < 0.05$, $**p < 0.01$, as measured by a two-tailed Student *t* test by comparison to untreated cells.

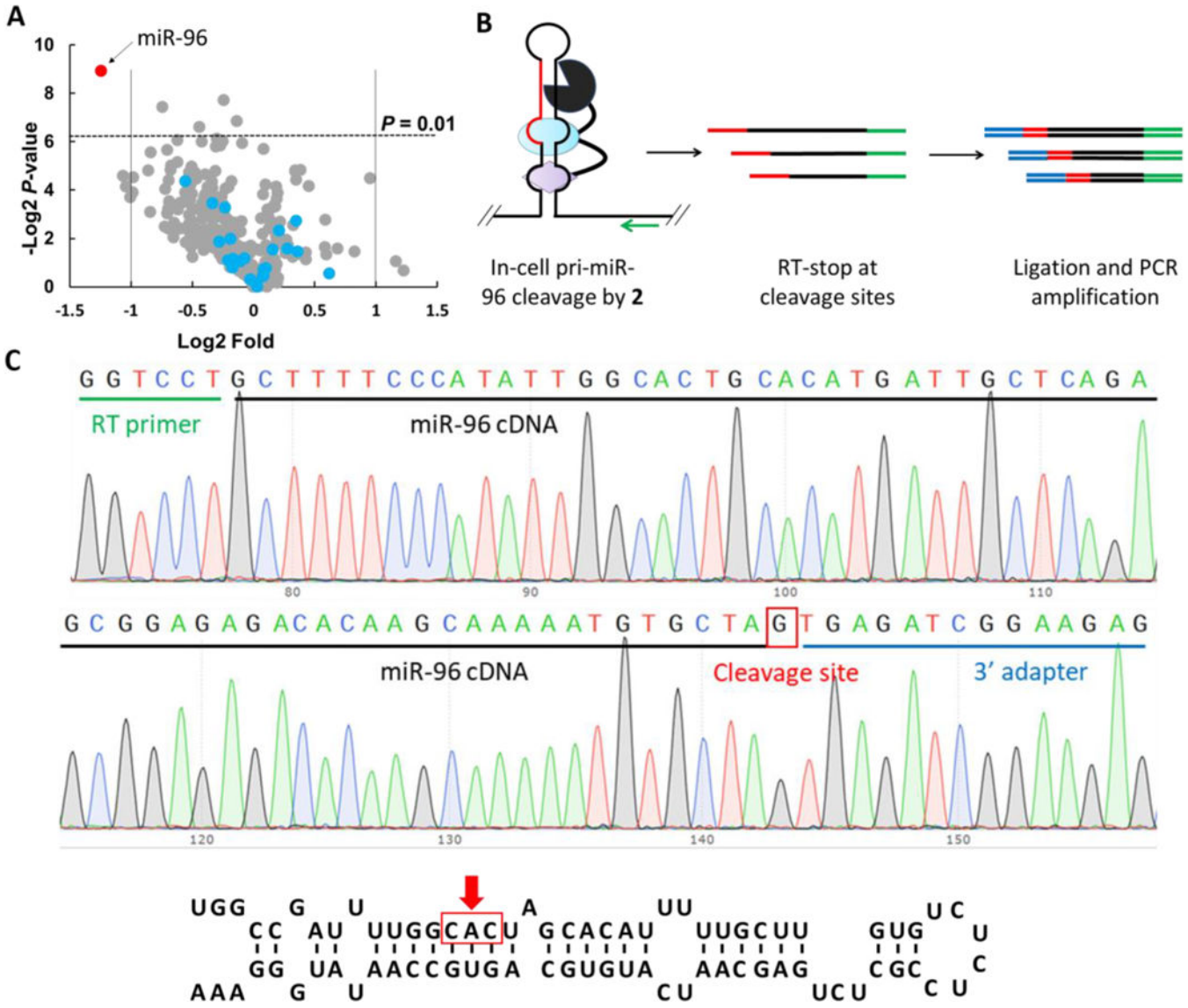

Figure 4.

An unbiased miRNA-profiling approach shows that **2** most significantly affects mature miR-96 levels in MDA-MB-231 cells, and amplification of cleavage products identifies the small molecule binding site within pri-miR-96. (A) Volcano plot for profiling the effect of **2** on all miRNAs expressed in MDA-MB-231 cells; miR-96 is the most affected (red, miR-96; blue, FOXOl-assoicated miRNAs or miRNAs with the same structures found in miR-96's Drosha site or the adjacent loop). (B) Scheme of the amplification approach to identify small molecule binding sites via cleavage. (C) Top, representative Sanger sequencing results from cDNA of the cleaved RNA. The cleavage site is indicated with a red box. Bottom, analysis of sequencing data revealed three cleavage sites (indicated with a red box and arrow in the pri-miR-96 secondary structure); ~40% of reads stop at the first C (5′); ~30% of reads stop at the A; ~30% of reads stop at the second C (3′). Data are expressed as mean ± SEM ($n \geq 3$).